LOAD RATING OF MASONRY AND CONCRETE ARCH BRIDGES

Thomas E. Boothby
Associate Professor,
Dept. of Architectural Engineering,
104 Engineering Unit-A,
Pennsylvania State University,
University Park, PA 16802
Phone: (814) 863-2082
Fax: (814) 863-4789
Email: tebarc@engr.psu.edu

Ece Erdogmus
Graduate Student,
Dept. of Architectural Engineering
104 Engineering Unit A,
Pennsylvania State University,
University Park, PA 16802
Phone: (814) 863-8313
Fax: (814) 863-4789
Email: exe132@psu.edu

ABSTRACT

Masonry and concrete arch bridges, for the most part built in the late nineteenth century and early twentieth century, are present in large numbers on the rail systems of the Northeastern United States. The owners of these structures often consider them prohibitively difficult to rate, and establish ratings based on engineering judgment. However, based on research from the UK and from the United States, the mechanics of these structures can be understood with a reasonable degree of confidence. In particular, it has been found that an adaptation of elastic frame analysis can provide reliable ratings of arch bridges for effects in the span direction. Critical transverse effects, such as pushing out or overturning of the spandrel walls or development of longitudinal cracks can be assessed using non-linear three-dimensional finite element analysis.

While Class-I railroads in Pennsylvania have been adopting a 315,000-pound maximum car weight rather than the previous 263,000 or 286,000-pound limits the load rating of arch bridges presents a particularly acute problem for short lines, as they decide whether to accept heavier car weight limits. For this purpose, a study for documenting the implication of the change in car weight limits on short line railroad bridges has been conducted for Pennsylvania Department of Transportation. Among the 1557 reported bridges on Pennsylvania short lines, there are 66 concrete arch and 147 masonry arch bridges. In this study a sample of 3 concrete and masonry arch bridges representing the whole population are analyzed and rated using recently developed non-linear three dimensional finite element tools. This study not only

describes the rating of the arch bridges according to the new weight limits but also shows that finite element analysis is a powerful tool for analyzing arch bridges, taking into account the material properties and interaction between the soil fill and concrete/masonry.

INTRODUCTION

Class-I Railroads across the United States and in Pennsylvania have been adopting heavier car weight limits, such as 315,000-pound cars rather than the previous 263,000 and 286,000-pound cars. Consequently, the short lines are in the dilemma of accepting or rejecting the operation of these heavier cars while the ratings for most of their bridges are not known. For this reason, a study called "Heavy Axle Study: Impact of Higher Rail Car Weight Limits on Short Line Railroads"(1) was carried out for the Pennsylvania Department of Transportation. The objective of this study was to calculate a statewide cost estimate for the upgrade of the under capacity infrastructure on the shortlines. There were 1557 bridges of several kinds in the database of the study, and rather than evaluating the entire population, a sample of 27 bridges was selected through a stratified random sampling method (1). Among the 27 bridges, three were filled arch bridges: one concrete and two masonry arches, as there were 66 concrete and 147 masonry arch bridges in the population. However, providing the evaluation of these filled arch bridges is not a common practice, as for other types of bridges. Filled arch bridges have been considered as difficult to rate compared to other types of bridges and for decades, they have been rated primarily based on engineering judgment. Nevertheless, recent studies have applied elastic frame analysis to the determination of the strength of arch bridges in the span direction (2), and the three-dimensional nonlinear finite element analysis method has been applied to the determination of transverse effects (3,4,5). In this study, results will be presented of two-dimensional elastic frame analysis and three-dimensional

nonlinear finite element analysis methods applied to three railroad arch bridges. The conventional railway bridge rating system will be adapted to suit the behavior of filled arch railroad bridges.

RAILWAY BRIDGE LOADING AND RATING SCHEMES

In this study, current and proposed car weight schemes are used for the objective of evaluating the bridges for these loadings. In order to provide a rating of these bridges, Cooper E-Loading schemes are also used. Cooper E-Loading has been used for railway bridges since late 19th century. The American Railway Engineering Association (AREA) has been adopting these schemes and offering as standard design and analysis loading schemes since the first version of the manual, "AREA 1905" (6). The current rating for bridges recommended by AREA is E80, although it represents a very high loading and none of the current car loadings rate as high as E80. Therefore, many short line bridges in the Heavy Axle Study (1) have been rated below E80 but are still able to carry the current car loadings.

ELASTIC FRAME ANALYSIS AND 2D RATING OF ARCH BRIDGES

The UK Experience

In the UK, the population of masonry arch bridges, both brick and stone, has been estimated at 50,000 or more, making this bridge easily the most common type of bridge. These bridges are widespread and dense on both the highway and rail transportation network, and the determination of their capacity, and the development

of repair methods has been critical. Since the 1940's, load rating of masonry arch bridges in the UK has been done by a semi-empirical method, developed at the time of World War II for rapid, unsophisticated assessment of the capacity of masonry arch bridges. This method, known as the MEXE (Military Engineering Experiment Establishment) method has been modified and codified for use in load-rating highway structures (7). Since the 1970's, it has been recognized, particularly because of growth in both highway and rail vehicle weights, that more rational and universal methods of bridge assessment are required. As a result, the Transport Research Laboratory carried out about a dozen full-scale ultimate strength load tests on redundant bridges, coupled with a program in the development of two-dimensional finite element analysis, and other methods for the rational analysis of arch bridges for assessment purposes (8).

This work contributed greatly to the ability to understand exactly how a masonry arch bridge can be expected to fail. In many cases, under a concentrated load applied over the full width of the bridge, the structure develops four hinges, and collapses as a two-dimensional mechanism (Figure 1). In these cases, it is possible to use mechanism analysis to estimate the collapse load of the structure and, with an appropriate safety factor on the loading, to establish a capacity for the structure. This is now a widespread method of assessment for arch bridges in the UK, and computer programs using this analysis and assessment method have been distributed (9).

However, two factors make the direct adoption of the mechanism method as an assessment tool in the US difficult. First, the use of the mechanism method

requires the application of limit states analysis, which is not taught as widely in the US as in the UK, and is not incorporated into design computer programs distributed in the US. Second, as demonstrated in the testing program in the UK, and as noted daily by inspectors of stone bridges in the US, in-service stone bridges do not only fail by the development of mechanisms in the span direction, but very often fail, or threaten failure, due to transverse effects. Soil pressures on the spandrel wall and wingwalls tend to overturn the spandrel walls, to push out the spandrel walls, or to cause the development of longitudinal cracks in the arch barrel. To overcome the first problem, an assessment method for arch bridges has been developed and validated, at least for highway bridges, that relies on elastic frame analysis, an analysis tool that is available to most bridge designers through widely distributed computer programs. The solution of the second problem will be described using the results of an investigation specific to railroad bridges, in which three-dimensional non-linear finite element analysis is used to identify the cause of observed transverse effects, and to assist in the identification of potential repair methods.

Arch Bridge Model

Frame

To model an elastic arch as a frame structure, it is necessary to divide the circumference into segments, and to identify nodal coordinates at the end of each of the segments. The nodes are joined by straight segments and fixed at the spring lines. Spring supports allowing horizontal translation, but not vertical displacement or rotation, are added at each of the supports, in view of the observed horizontal

displacements in a field testing program, described in a previous publication (10). It was found that ten segments around the circumference of the arch, as recommended by BA 16/97 (7), are sufficient to capture the behavior of the arch ring. The geometry of the frame representing the arch ring is shown in Figure 2.

Properties

Appropriate member material properties for entry into the frame analysis program have been determined by analysis of field data, finite element results, and consultation with literature on stone masonry and concrete construction. The cross sectional area and moment of inertia are based on the geometry of a unit (1 ft) width of the arch ring, discounting the effects of spandrel walls, fill, and haunching. Neglecting the strengthening and stiffening effects of these features is conservative from the point of view of load rating. The fundamental material stiffness property used in the analysis is an effective modulus of elasticity representing the combined effect of masonry units, mortar, and joints. The resulting modulus of elasticity is significantly lower than the modulus of elasticity of the units alone, reflecting the general use of soft mortars in the construction of arch bridges. Elastic spring stiffnesses are input for the horizontal supports at the abutments and interior piers. The stiffness constants used are based on matching the field data and analytical results. Abutment spring stiffnesses are generally greater than pier spring stiffnesses; due to the passive earth pressure of the approach fill material. In the absence of apparent flaws, railroad masonry is generally carefully and consistently cut and placed. Relatively high values of modulus of elasticity (2,000,000 to 5,000,000 psi),

compressive strength (1000 to 2000 psi), and tensile strength (50-150 psi) may be depended on. Spring constants of 5000-10000 kips/in maybe used at abutments, with half the abutment value to be used at interior piers in multi-span bridges.

Loads

The self-weight of the arch ring is computed accurately by most analysis programs, given the cross sectional area and density of the material of the arch ring. Dense stone weighs 160 lb/ft^3, and concrete weighs about 150 lb/ft^3 so these values are used consistently for the self-weights of the arch ring. Superimposed dead loads include the weight of the fill and the weight of the paving material. The superimposed load on an arch segment is taken to be the total weight of the segment of fill and paving lying above the element, uniformly distributed over the element. The geometry of this segment is illustrated in Figure 2. The weight of the segment, given a unit width of arch ring, is the area of the segment times the unit density. The unit density is taken as 120 lb/ft^3–a reasonable value for soil materials. The live load is taken as a linearly varying vertical pressure on both directions on the back of the arch ring resulting from a rail car wheel load converted to a pressure distribution under the ballast according to the equations recommended by the AREA specifications, 1996 (11). The pressure due to the wheels of an E-Loading distributed through the ballast and the soil fill is calculated at the elevation of the nodal points, based on a three dimensional pyramidal distribution, as illustrated in Figure 3. The total pressure at the bottom of the ballast is applied over a length of 36 in, which is equivalent to the diameter of one wheel according to AREA. The load is assumed to be dispersed

through the fill at a slope of 2 vertical to 1 horizontal in both directions. This procedure is similar to that given in BA 16/97 ((7). The application of the live load, then, involves the determination of the depth of the fill above each of the nodes of the arch ring segment, the determination of the wheel load pressure at each of the nodes, and the assumption of a linearly varying pressure from one node to the other.

Comparison of Proposed Analysis to Field Test Results

Four bridges in the field-testing program described in previous studies (10, 12) were modeled under the actual loading of the test program for comparison of results. The results are compared based on the profile of an entire span of the arch under a single load placement. A complete summary of the comparison of field data to frame analysis results is available (12) and further comparison between this method and results of field-testing have been made (2).

Calculation of Arch Ring Capacity

The output from a frame analysis can be used to compare to the capacity of masonry or concrete. The capacity of the masonry/concrete of the arch ring subjected to combinations of axial force and moment can be considered linearly elastic or elastic-plastic, and the assessment can include or omit a small tensile capacity. In every case, it is reasonable to allow cracking in the masonry/concrete. Figure 4 compares the four possible limit states for the arch ring.

Previous studies, (4, 5,10) demonstrate that the masonry must be considered capable of carrying a limited tensile stress to assure fidelity to experimental results

and accuracy of bridge assessment. In this study two ultimate strength models are considered: no tension and tension allowed. The ultimate strength, cracking allowed, tensile stress allowed is presented as the preferred alternative for calculating the strength of masonry and concrete arch rings.

The interaction diagrams for each of the two models can be calculated by the following procedure:

1. Ultimate Strength, cracking allowed, no tensile stresses as illustrated in Figure 4(b) leads to the following equation:

$$f_c = \frac{P}{h - 2e} \tag{1}$$

Where P is the axial force, e=M/P, h is the thickness of the arch ring, and f_c is the maximum compressive stress. Given M and P at a cross section, f_c can be readily calculated and compared to a maximum permitted value.

2. The explicit calculation of the ultimate strength, tension allowed condition is not so straightforward. From force equilibrium on the stress diagram on Figure 4(d), the quantity a , representing the ratio of compressive stress block depth to overall depth can be found

$$a = \frac{P + bf_c h}{f_c h(1 + b)} \tag{2}$$

where b is the ratio of tensile strength to compressive strength. Moment equilibrium then yields

$$f_c = \frac{2}{ah^2} \frac{M}{(1 - a)(1 + b)} \tag{3}$$

By eliminating a between the two equations, an explicit quadratic equation for f_c is obtainable. Then the explicit expression for f_c is:

$$f_c = \frac{1}{2b\,h^2}\left[\sqrt{[Ph(1-b)-2M(1+b)]^2+4b(Ph)^2}-[Ph(1-b)-2M(1+b)]\right] \quad (8)$$

Determination of Load Rating

The load rating of a structure is determined by comparing the critical dead and live load axial thrust and moment at each node of a structure, as calculated by elastic frame analysis, to the maximum axial thrust moment envelope developed using the procedure in the previous section. The maximum stress (f_c) to be used in the equations can be determined by testing material removed from the structure or, in the absence of such tests, by using empirical values developed from the results of the present testing program. The moments and axial thrusts used in the analysis result from the application of an E80 or higher loading to a critical position on the structure.

Concrete Arch Short Line Railroad Bridge

As an application of the procedure of elastic frame analysis and load rating procedure described so far, a concrete arch railroad bridge is analyzed and load rated. The bridge will be designated as Bridge #3, is a single span concrete arch bridge built in 1920's. It is a 39 ft span, 32 ft high bridge with a span/rise ratio of 0.8. It has a 13 ft embankment on top of the arch barrel. The thickness of the arch barrel is found to be as 36 inches based on the site observations. The Class-3 track structure on the bridge has 132RE standard rail and the limiting operating speed by Federal Railway

Administration is 40 mph. The material properties used for the analyses are based on previous literature and AREA, 1996 (11) where the modulus of elasticity is taken as 3,000,000 psi and the compressive strength as 2,000 psi. The low compressive strength of the concrete is selected based on the poor condition of the spalling concrete and the construction date of the bridge. Following the procedure of load rating discussed previously and constructing the necessary interaction diagrams, it is seen that this bridge is capable of handling E80 loading when the ultimate strength, cracking allowed, tensile stress allowed limit state is used (Figure 5). To find the rating of the bridge, the E-loading is increased until this limit state is reached at a load around E600 (Figure6). Therefore, in terms of strength in the span direction, this concrete arch bridge rates at about E600. A suitable safety factor of 2-3 would have to be applied to this analysis, resulting in a rating of E200-E300.

However, when the necessary calculations are carried out for the track structure according to AREA recommendations, it is observed that the bridge should not carry beyond E80 loading. Moreover, as will be seen in the next section, the transverse strength of the bridge changes the rating of the bridge considerably.

APPLICATION OF 3D FINITE ELEMENT ANALYSIS METHOD

A recently developed three-dimensional nonlinear finite element method has been validated by comparison to field-test results and has been observed to make accurate predictions of the transverse behavior of the arch bridges (3,4,5). It has also been observed that the transverse effects on concrete or masonry arch bridges such as

pushing out or overturning of the spandrel walls or longitudinal cracks in the arch barrel are at least equally important to the effects in the span direction and may lead to failure. Moreover, in railroad bridges with high embankments, the transverse effects appear to be particularly important due to the very large soil pressures developed by the embankments. On these bridges, the concentrated loads at the top of the embankment are distributed though the deep soil fill and are transferred to uniform pressures on the arch barrel, resulting in a favorable loading condition in the span direction.

Three shortline railroad arch bridges were analyzed with the nonlinear finite element analysis model by using the software package ANSYS 5.6 and the results will be discussed here briefly.

Bridge #1

This bridge has nearly 40 feet of soil fill and embankment mass on top of the bridge. However, the span is 10 feet, which is relatively very short. The stresses due to loading are distributed through all the soil fill volumes and are transformed to uniformly distributed-loads on the arch barrel. Therefore, it is clear that the changes in the wheel loads applied to the top of the embankment will not create any dramatic effects on the arch. In order to understand the accuracy of this prediction, a simplified soil model was developed. In this model the entire embankment volume is modeled in real dimensions but rather than modeling the arch barrel and spandrel walls directly, a retaining wall representing the spandrel walls is modeled. Since all the features are symmetric about the vertical axis, only half of the structure is modeled using

symmetry boundary conditions on the cut surface (Figure 7). The boundary conditions simulating the buttressing effects of the wing walls are added to the model in the longitudinal and transverse directions. The base of the spandrel wall is constrained at all displacement degrees of freedom. The base of the embankment is also restrained for vertical and longitudinal but no transverse displacements, similar to plane strain conditions. The model was analyzed first under gravity and the maximum stress created on the bridge was 287 psi. Then live loads were applied, including 263, 286 and 315 kip cars. The resulting maximum stresses were 301, 303 and 302 psi respectively. The 286 kip car ended up being the worst case, because it has higher wheel loads than 263 kip car but has the same axle spacing. The 315 kip car has much higher wheel loads but the spacing of the axles is also increased, decreasing the cumulative effect of the wheels. However, the main effect on the bridge is created by the dead load in this case and the effect of the load change at the top of the embankment has only a very small effect at the level of the arch structure.

Bridge #2

This bridge also has a high embankment on top (8 feet). The bridge is asymmetric in every direction requiring the use of a full model. This bridge has already undergone a collapse of the downstream spandrel wall. Instead of being repaired, timber cribbing was provided to prevent further sloughing of the fill. In order to determine the strength of the remainder of the bridge it was necessary to take the collapsed spandrel wall out of the model, adjust the slope of the fill accordingly, simulate the timber cribbing by appropriate boundary conditions and run the program

with these configurations; an actual simulation of the defective structure. The timber cribbing was modeled by additional transverse constraint to the fill at the location of the cribbing.

The modified model was analyzed under the 263,000-pound, 286,000-pound, 315,000-pound cars with a tensile strength value of 125 psi. The results show that the upstream spandrel wall collapsed under the car loadings. As the loads were added incrementally in this procedure, the spandrel wall collapsed at 35 -40% of all three-car loadings. The deflected shape is shown in Figure 8. When the actual spandrel was inspected on site, cracks were observed in the same area as finite element analysis results show. Therefore, a repair scheme consisting of removing some portion of the fill to decrease the thrust on the spandrel wall was recommended.

Bridge #3

The third bridge analyzed is the concrete arch bridge, which has also been rated by the elastic frame analysis method discussed in the previous sections. The spandrel walls are restrained laterally by diagonal wing walls on three corners but on the fourth corner, a retaining wall making an 180º angle with the spandrel wall. There is no restraint in the transverse direction on this corner. This asymmetry in the geometry led to the creation of a full model. Boundary conditions for horizontal restraint on the three corners are provided, to simulate the angled wing walls.

The results of the analyses carried out for the model described, show that this bridge can resist the current and proposed car loadings or greater loads. The maximum deflection was found on the upper corner of the spandrel wall with

asymmetric wing wall configurations. The deflected shape is shown in Figure 9. When the bridge was loaded up to collapse by the incrementally increasing E-loadings, the unrestrained spandrel wall collapsed and dragged some of the arch barrel creating a failure on the interface between the arch barrel and the spandrel wall at a load level of E190. The cracks created at the failure load of E190 and the similar cracks observed on site are shown in Figure 10. Again, the application of a safety factor of 2-3 to this structure produces a rating of E65-E95 although the bridge can comfortably support 315 kip car loading.

CONCLUSIONS

In this study, two masonry and one concrete arch bridge selected from the entire population of shortline railroad bridges in Pennsylvania were analyzed to document the influence of recently proposed heavy axles on short line railroad arch bridges and two different methods of analysis were employed for this purpose.

The previously validated method of elastic frame analysis is a quick, simple and reasonably accurate means of assessing these bridges in the span direction. It is a very efficient way of observing the arch barrel behavior under the different live load schemes and influence of the dead load of the high embankments. However, as transverse behavior is particularly important for the railroad bridges, it is necessary to supplement this method with an analysis effective in the transverse direction. The three-dimensional finite element analysis method, also validated previously, determines the load effects created in the span direction as well the transverse direction. The collapse of one spandrel wall in Bridge #2, and the failure of the

spandrel walls of Bridge #3 under high E-loadings show the importance of transverse effects on railroad bridges with high-embankments.

As a result, of the analyses, the proposed 315 kip cars were found to be acceptable for two of the three bridges. However, one bridge, which has already undergone a spandrel wall failure, needs repair and improvement to be able to carry the 315 kip car loading safely.

ACKNOWLEDGEMENTS

The research presented in this paper was sponsored by PennDOT Bureau of Rail, Freight, Port and Waterways in PennDOT and the National Science Foundation, Award No. CMS-9642614. The authors also gratefully acknowledge the assistance of Sally Gimbert.

REFERENCES

1. Laman, J.A., Gittings, G.L., Boothby T.E., Leighty, C., Erdogmus, E. "Heavy Axle Study: A Statistical Assessment of Railroad Infrastructure," PTI Report to be published in August 2001.
2. Boothby, T. E., "Load Rating of Masonry Arch Bridges," *Journal of Bridge Engineering*, Vol.6, No.2, 79-86.
3. Roberts, Benjamin J. (1999). *Transverse Behavior of Masonry Arch Bridges*. M.S. Thesis, The Pennsylvania State University.
4. Fanning, P.J. and Boothby, T.E. and Roberts, B.J. (2001). "Longitudinal and Transverse Effects in Masonry Arch Assessment," *Construction and Building Materials*, Vol.15, 51-60

5. Fanning, P.J. and Boothby, T.E., "Three Dimensional Modelling And Full-Scale Testing Of Masonry Arch Bridges," to appear, *Computers and Structures*, 2001.

6. American Railway Engineering Association (1905), Manual for Railway Engineering.

7. Department of Transport, U. K. (1993). "The assessment of highway bridges and structures." Advice note BA 16/93, Her Majesty's Stationery Office, London.

8. Page, J. (1995). "Load Tests to Collapse on Masonry Arch Bridges," *Arch Bridges*, Thomas Telford, London, 289-298.

9. OBVIS, Ltd. (2001). "ArchieM Quick Guide," Exeter, UK, OBVIS Ltd.

10. Boothby, T.E., Domalik, D.E., & Dalal, V.A. (1998). "Service Load response of Masonry Arch Bridges." *Journal of Structural Engineering*, ASCE, 124 (1), 17-23.

11. American Railway Engineering Association (1996). Manual for Railway Engineering

12. Boothby, T.E., Domalik, D.E., & Elgin, C.S. (1997). "Load Rating of Masonry Arch Bridges and Culverts." *Res. Rep. No. FHWA/OH-96/016.(Nat. Tech. Infor. Service No. PB-97-1485555)* Ohio Department of Transportation, Columbus, Ohio.

FIGURE CAPTIONS

Figure 1- Mechanism of an Arch Bridge under Concentrated Load

Figure 2- Arch Ring Subdivision

Figure 3-Live Load Distribution

Figure 4- Various Models of Masonry Arch Ring Limit States

4(a) Service load, cracking allowed, no tensile stresses

4(b) Service load, cracking allowed, tensile stresses

4(c) Ultimate strength, cracking allowed, no tensile

4(d) Ultimate Strength, cracking allowed, tensile

Figure 5- E-Rating Plot for E80 loading, Concrete Arch Bridge

Figure 6- E-Rating Plot for E600 loading, Concrete Arch Bridge

Figure 7- Half-Soil Model for Bridge #1

Figure 8- Deflected shape and Collapse on Bridge #2 (f'_t=125 psi)

Figure 9- Deflected Shape of Bridge #3 under 315k Car Loading

Figure 10- Arch Barrel Spandrel Wall Separation and Longitudinal Cracks in the Arch barrel

FIGURES

Figure 1

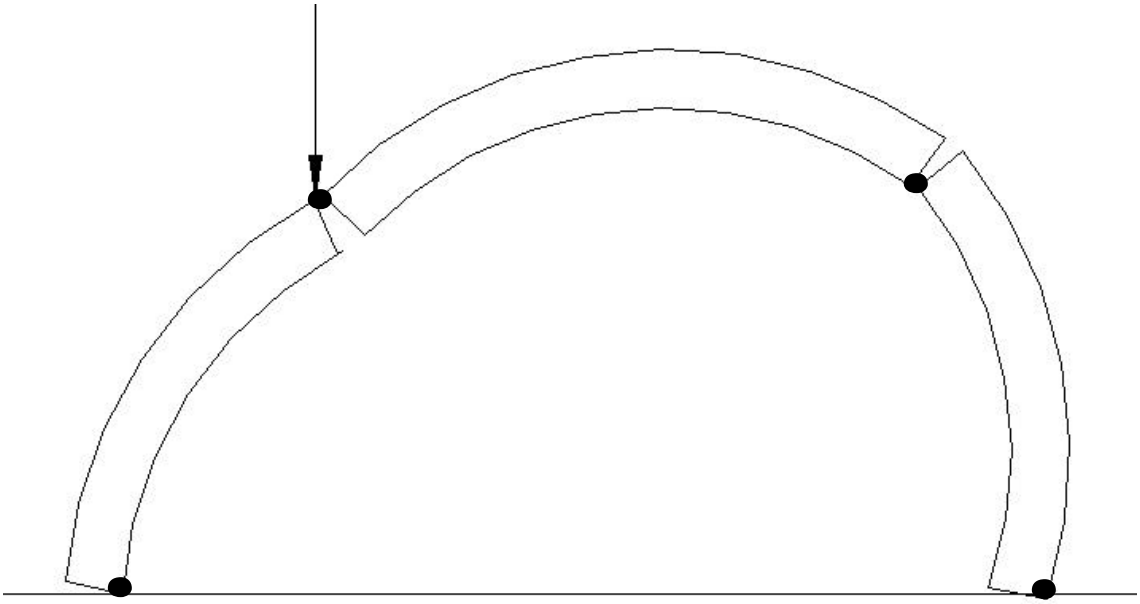

Figure 1- Collapse Mechanism of an Arch Bridge under Concentrated Load

Figure 2

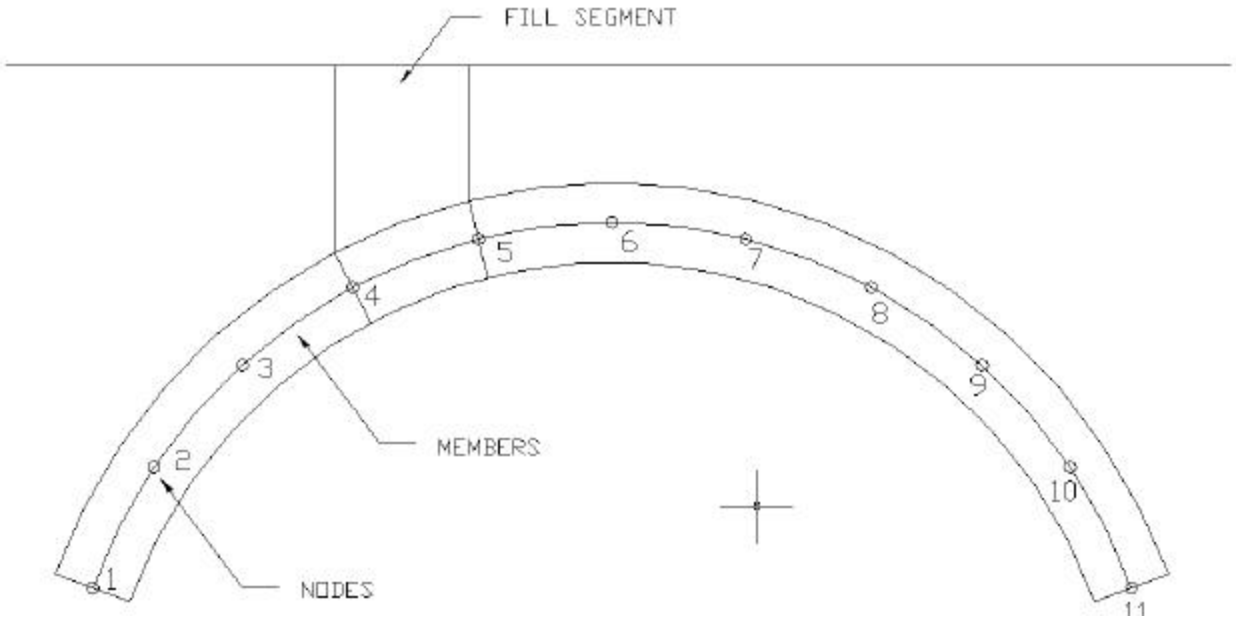

Figure 2- Arch Ring Subdivision

Figure 3

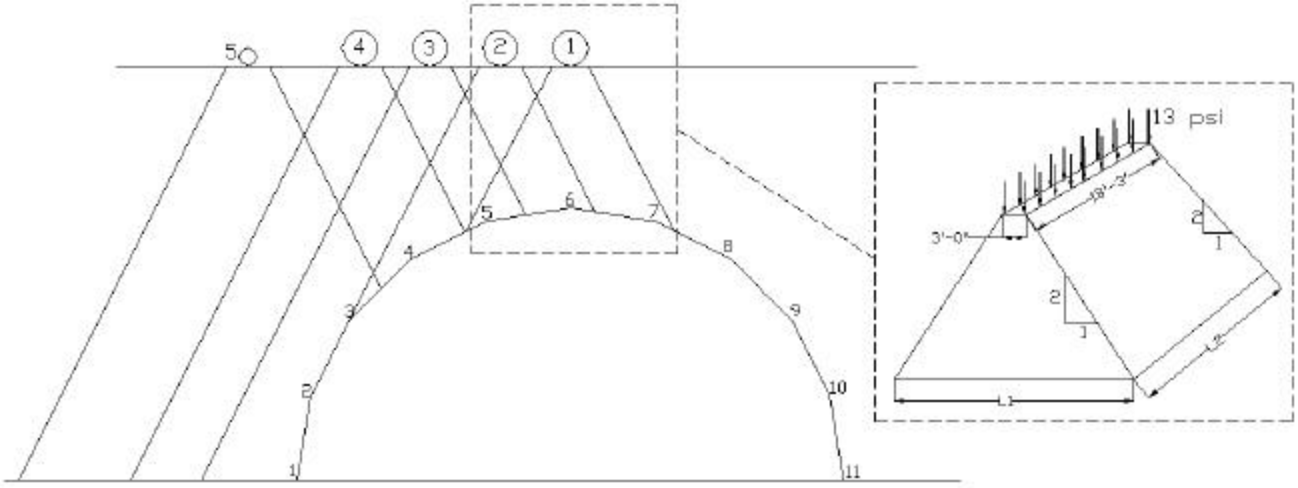

Figure 3-Live Load Distribution

Figure 4

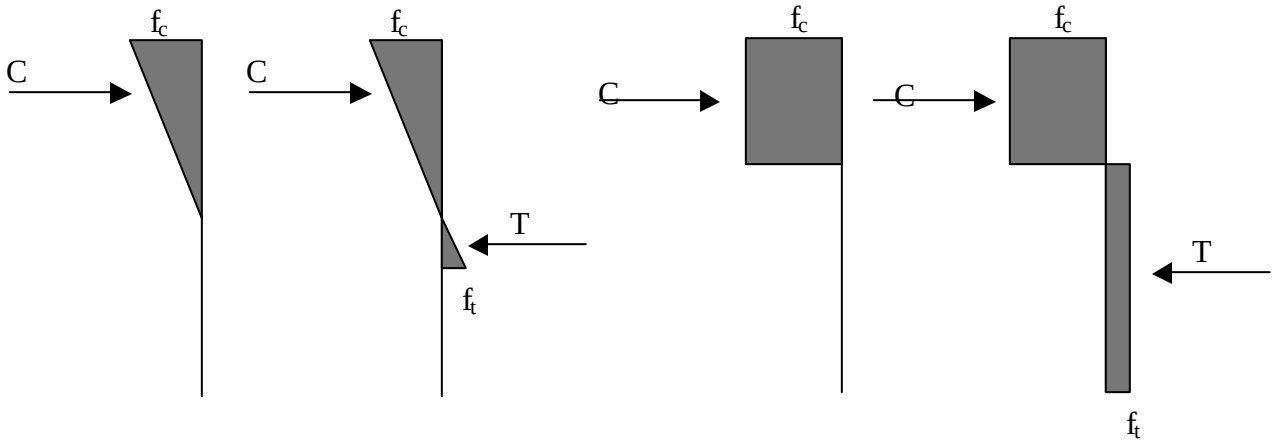

(a) Service load, cracking allowed, no tensile stresses

(b) Service load, cracking allowed, tensile stresses

(c) Ultimate strength, cracking allowed, no tensile

(d) Ultimate Strength, cracking allowed, tensile

Figure 4- Various Models of Masonry Arch Ring Limit States

Figure 5

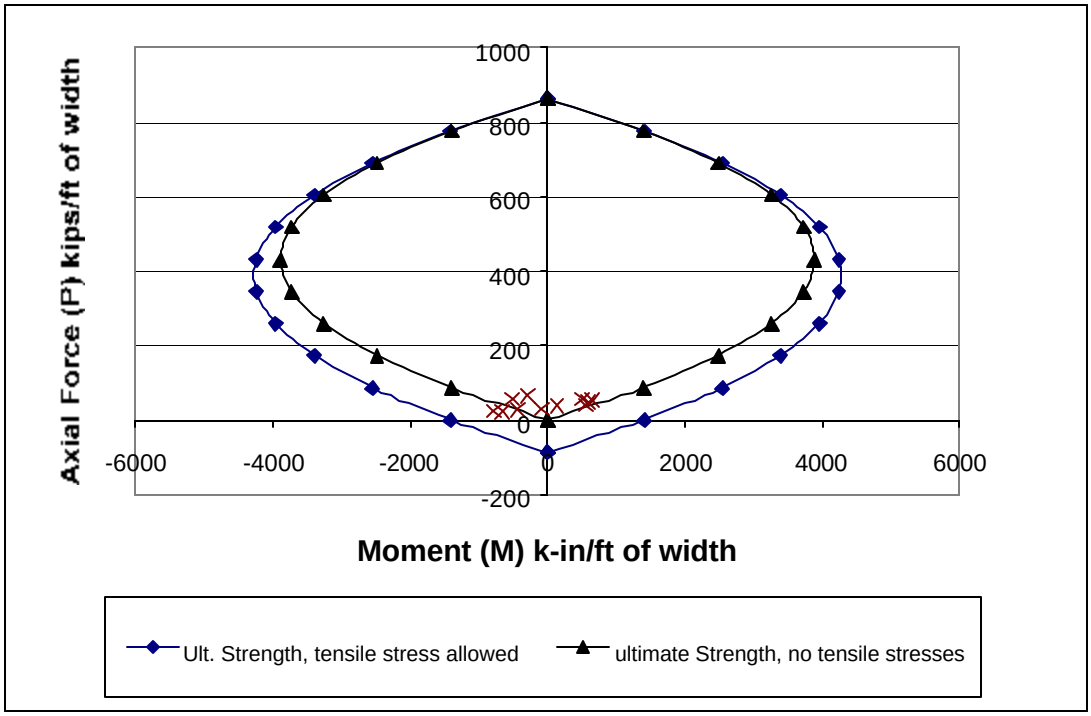

Figure 5- E-Rating Plot for E80 loading, Concrete Arch Bridge

Figure 6

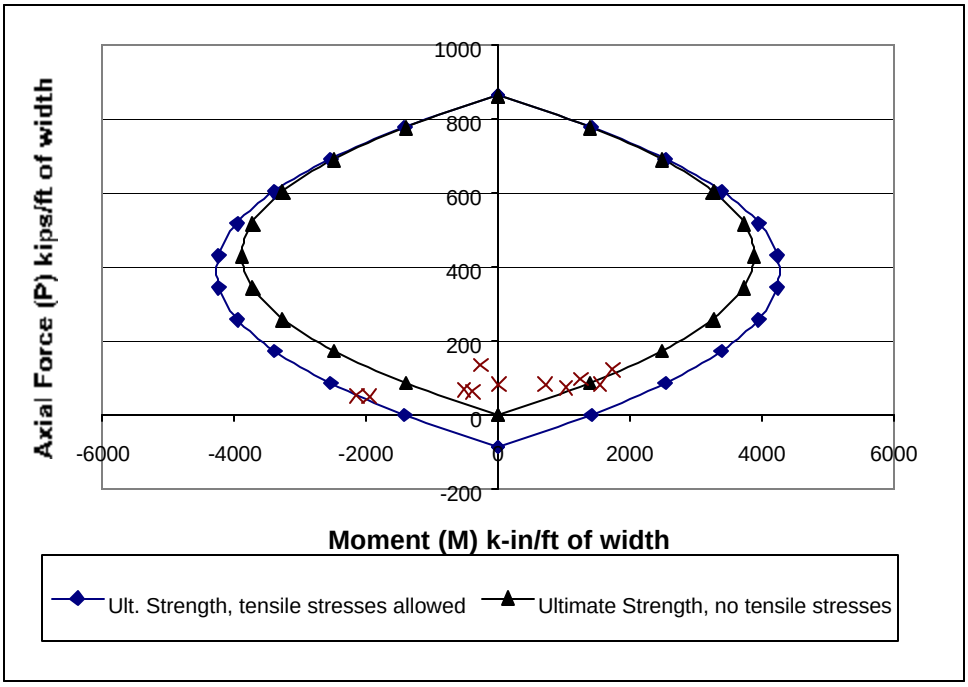

Figure 6- E-Rating Plot for E600 loading, Concrete Arch Bridge

Figure 7

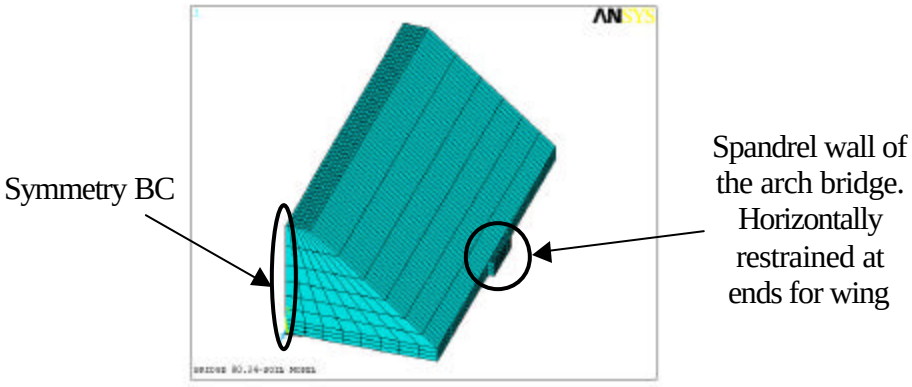

Figure 7- Half-Soil Model for Bridge #1

Figure 8

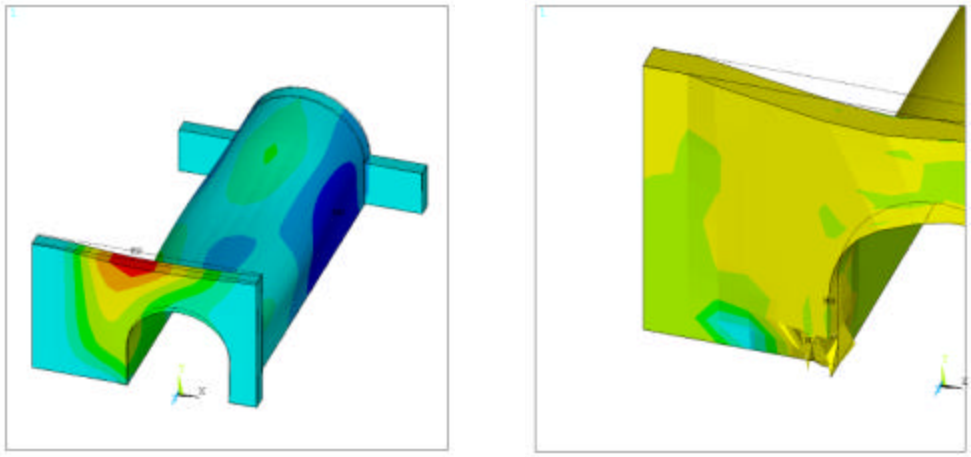

Figure 8- Deflected shape and Collapse on Bridge #2 (f'_t=125 psi)

Figure 9

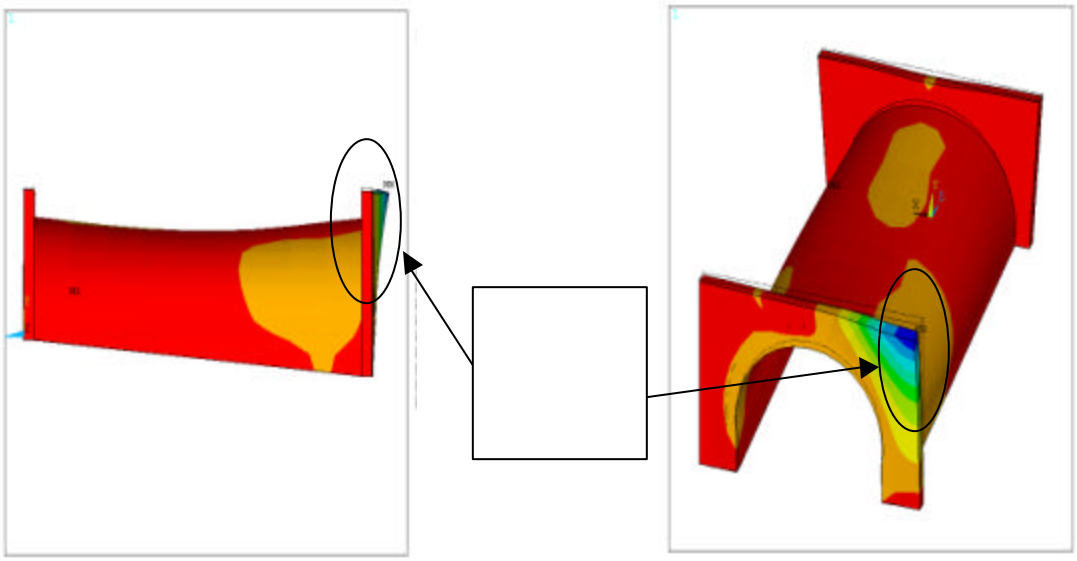

Figure 9- Deflected Shape of Bridge #3 under 315k Car Loading

Figure 10

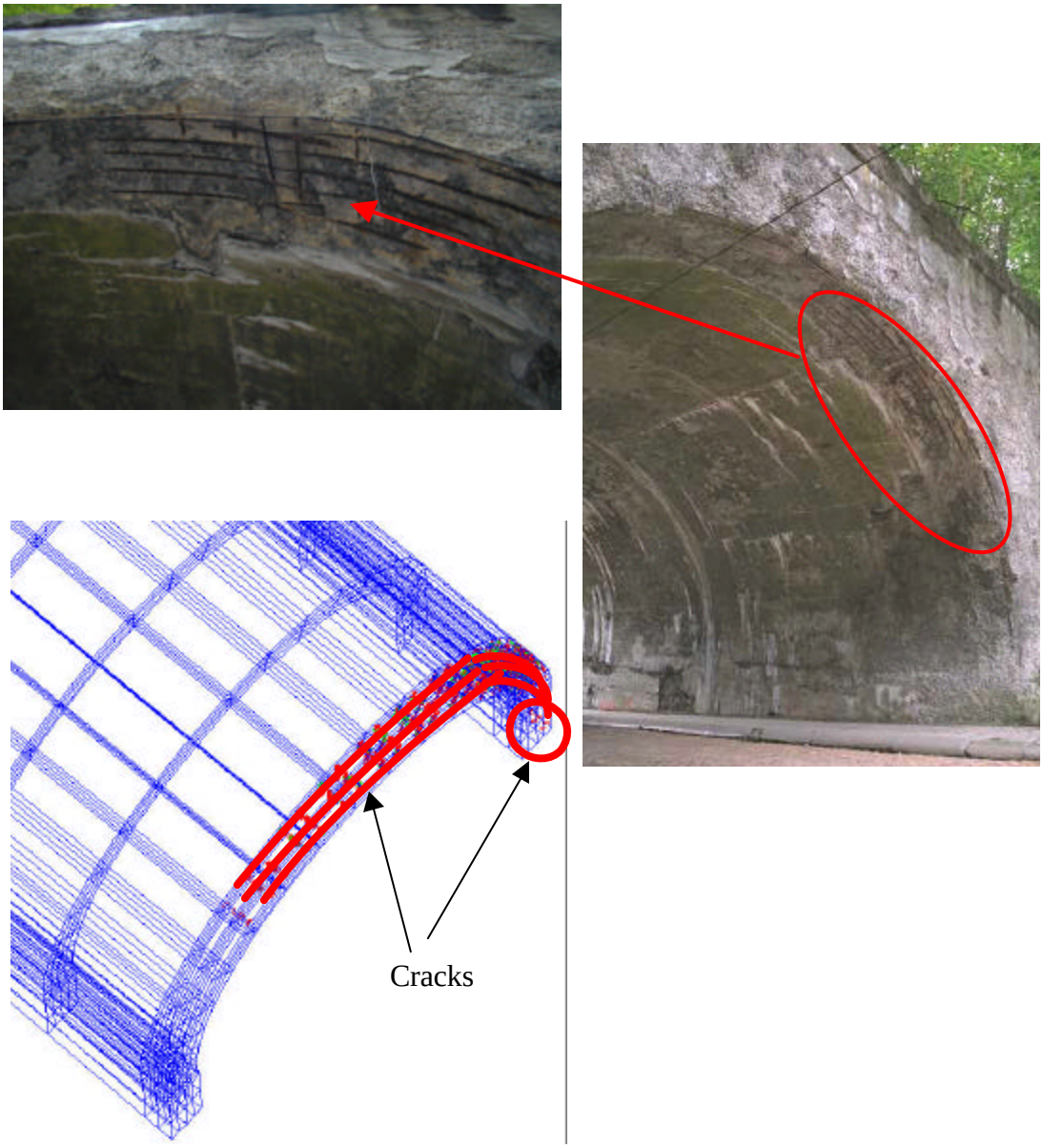

Figure 10- Arch Barrel Spandrel Wall Separation and Longitudinal Cracks in the Arch barrel